Polyethylene nanofibres with very high thermal conductivities

Sheng Shen[1], Asegun Henry[1], Jonathan Tong[1], Ruiting Zheng[1,2] and Gang Chen[1]*

Bulk polymers are generally regarded as thermal insulators, and typically have thermal conductivities on the order of 0.1 W m^{-1} K^{-1} (ref. 1). However, recent work[2-4] suggests that individual chains of polyethylene—the simplest and most widely used polymer—can have extremely high thermal conductivity. Practical applications of these polymers may also require that the individual chains form fibres or films. Here, we report the fabrication of high-quality ultra-drawn polyethylene nanofibres with diameters of 50–500 nm and lengths up to tens of millimetres. The thermal conductivity of the nanofibres was found to be as high as ~104 W m^{-1} K^{-1}, which is larger than the conductivities of about half of the pure metals. The high thermal conductivity is attributed to the restructuring of the polymer chains by stretching, which improves the fibre quality toward an 'ideal' single crystalline fibre. Such thermally conductive polymers are potentially useful as heat spreaders and could supplement conventional metallic heat-transfer materials, which are used in applications such as solar hot-water collectors, heat exchangers and electronic packaging.

Typical methods for improving polymer thermal conductivity have often focused on composite materials, in which additives such as metallic nanoparticles or carbon nanotubes are embedded in polymer matrices[5,6]. In particular, the use of carbon nanotubes as the additive has been motivated by reports that individual tubes have high thermal conductivities[7]. The enhancement of thermal conductivity in polymer carbon nanotube composites is usually limited to within one order of magnitude due to the high thermal interface resistance between the additives and the polymer matrix[8,9].

The alignment of polymer chains, however, can result in a large enhancement of the mechanical strength and thermal conductivity of polymers[10,11]. In the limit of an individual polyethylene chain, illustrated in Fig. 1a, theoretical predictions suggest that a very high (~350 W m^{-1} K^{-1}) or even divergent thermal conductivity can be achieved[4], consistent with the non-ergodic characteristics of one-dimensional conductors originally studied by Fermi, Pasta and Ulam[12]. Several experimental studies have shown that self-assembled monolayers of aligned polyethylene chains also show a very high thermal conductance[2,3]. In bulk polyethylene, however, the defects (polymer chain ends, entanglement, voids, impurities and so on; Fig. 1b) all act as stress concentration points and phonon scattering sites for heat transfer[13]. As a result, bulk polyethylene has low strength and low thermal conductivity. For many years, it has been well known that the mechanical and thermal properties of polyethylene can be improved by processing or stretching bulk samples into thin films or fibres to reduce the number of defects and increase the chain alignment[14,15]. Commercial oriented polyethylene fibres, with diameters ranging from 10 to 25 μm (Fig. 1c), have been found to have an enhanced Young's modulus of ~200 GPa and a thermal conductivity of 30–40 W m^{-1} K^{-1} at around room temperature[16,17]. To further reduce the number of defects, we scaled down the fibre size and developed a new method to fabricate ultra-drawn nanoscale fibres (Fig. 1d). The thermal conductivity of these nanofibres was as high as 104 W m^{-1} K^{-1}, which is larger than many metals.

Our technique to fabricate high-quality ultra-drawn polyethylene nanofibres uses a two-stage heating method (see Supplementary Information). The fibres are created from a polyethylene gel prepared by dissolving 0.8 wt% ultrahigh-molecular-weight polyethylene (molecular weight, 3–6 × 10^6; Alfa Aesar) powder in decalin at 145 °C under nitrogen. The solution is then quenched in water to form a gel. Subsequently, a small sample of wet gel is heated to 120 °C on a heating stage and an individual suspended fibre is drawn from the heated gel using either a sharp tungsten tip (diameter, ~100 nm) or a tipless atomic force microscope (AFM) cantilever[18,19]. This is conducted under the direct view of an optical microscope using dark-field illumination. A second heating procedure is then used to heat the fibre and surroundings to ~90 °C to dry the fibre. The fibre is then mechanically stretched (ultra-drawn) at a controllable speed by rigidly fixing the tungsten tip or AFM cantilever to a motorized control stage.

The overall draw ratios were estimated to be between 60 and 800 (see Supplementary Information), but the straining was non-uniform along the fibre length such that the region closest to the tip experienced a higher level of deformation than the region closer to the heated gel. The region of the fibre that was used in subsequent thermal conductivity measurements was taken from the most necked region, obtained by mechanically cutting the drawn fibre. This section was expected to have the highest deformation. Most of the fabricated nanofibres had uniform diameters between 50 and 500 nm and lengths up to tens of millimetres. Figure 1e,f shows a transmission electron microscope (TEM) micrograph and diffraction pattern for one sample of our ultra-drawn polyethylene nanofibres fabricated by a tungsten tip. The periodic diffraction spots could be distinctly indexed to an orthorhombic phase with lattice constants $a = 7.422$ Å, $b = 4.949$ Å and $c = 2.544$ Å for polyethylene[20]. The arrow in Fig. 1f indicates the drawing direction. This pattern shows the strong single-crystal nature of the fabricated polyethylene nanofibres, with the c-axis (molecular) aligned with the drawing direction and the a-axis normal to the fibre axis. This confirms that the stretching effect (ultra-drawn) in the nanofibres (Fig. 1e) does indeed contribute to the nanoscale restructuring of the polymer chains, with the improvement in fibre quality leading to more 'ideal' single-crystalline fibres (Fig. 1d).

To measure the thermal conductivity of an individual nanofibre, we have developed a general approach for thermal measurements of compliant nanofibres or nanowires using a sensitive bi-material

[1]Department of Mechanical Engineering, Massachusetts Institute of Technology, Cambridge, Massachusetts 02139, USA, [2]Key Laboratory of Radiation Beam Technology and Materials Modification of Ministry of Education, College of Nuclear Science and Technology, Beijing Normal University, Beijing, 100875, China. *e-mail: gchen2@mit.edu
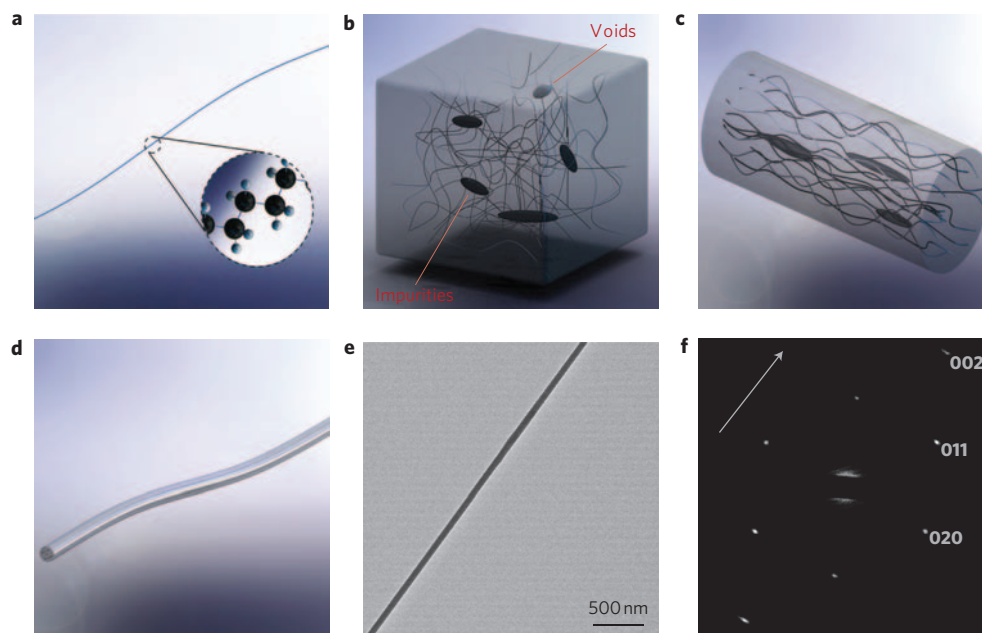
251

Figure 1 | Polyethylene chains and fibres. a, Illustration of one single molecular chain of polyethylene. The inset shows the chemical structure of polyethylene (carbon atoms are shown in black, hydrogen atoms in white). **b,** Bulk polyethylene containing chain ends, entanglements, voids and defects. **c,** Stretched polyethylene microfibre. **d,** 'Ideal' polyethylene nanofibre with perfectly aligned molecular chains. **e,** TEM image of an ultra-drawn polyethylene nanofibre. **f,** TEM diffraction image of the ultra-drawn polyethylene nanofibre. The arrow represents the drawing direction.

AFM cantilever, which can resolve power measurements as low as 0.1 nW and energy measurements down to 0.15 pJ (refs 21,22). Our experimental set-up is presented in Fig. 2. A nanofibre is directly drawn by a tipless bi-material (Si_3N_4/Au) AFM cantilever, which minimizes the thermal contact resistance between the fibre and the cantilever. The nanofibre is then mechanically cut ~300 μm away from the tip to reduce radiation loss from the fibre to the environment. Note that we have estimated this radiation
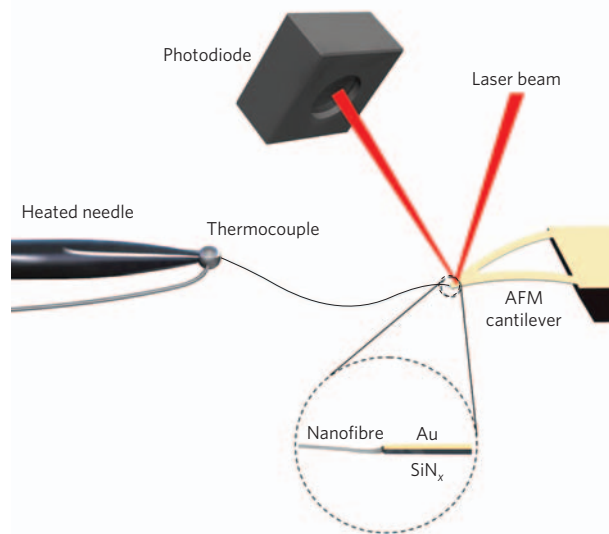

Figure 2 | Schematic of experimental set-up used to measure the thermal properties of a single ultra-drawn nanofibre. The thermal sensor is a silicon nitride AFM cantilever coated with a 70-nm gold film. A laser beam (wavelength, 650 nm; output power, 3 mW) is focused on the tip of the cantilever and reflected onto a bi-cell photodiode. The nanofibre drawn from the AFM cantilever is loosely suspended between a micro thermocouple and the AFM cantilever.

loss and verified that it can be neglected. The set-up is then placed under high vacuum (~50 μtorr). A laser (wavelength $\lambda = 650$ nm) is focused onto the tip of the cantilever and reflected onto a bi-cell photodiode, which measures the deflection of the cantilever. The free end of the fibre is attached with conductive silver epoxy to a micro thermocouple (junction diameter, ~50 μm), which is mounted onto the tip of a steel needle. Its temperature can be adjusted by heating the needle with a small electrical resistance heater. By varying both the laser power and the temperature of the micro thermocouple, we can determine the polyethylene nano-fibre conductance by measuring the deflection of the cantilever (see Supplementary Information). To eliminate the effect of thermal expansion, a motorized control stage was used to reduce the distance between the cantilever and the thermocouple until the nanofibre was no longer under tension (Fig. 2), which was indicated by the point at which the deflection signal stopped changing with further stage movement. We were not successful in measuring polymer fibres with diameters in the micrometre range, because they are too stiff, with the cantilever deflection affected by the thermal expansion of the fibres.

In the first step of the experiment, we calibrated the bending of the cantilever by varying the laser power (Fig. 3a). Because the thermal conductance of the cantilever is ~1,000 times larger than that of the fibre[23], almost all of the absorbed laser power will conduct to the base of the cantilever, with ~0.1% of the absorbed heat conduct-ing through the nanofibre. In the second step, we held the laser power constant and varied the temperature at the thermocouple. The heat conducted across the nanofibre changes in response to the changing temperature difference between the cantilever and the thermocouple. Before varying the thermocouple temperature, the initial bending of the cantilever is fixed at a given laser power and is thus used as a zero reference. Because this measurement is intrinsically differential, we can measure minute changes in the heat conducted through the nanofibre. Thus, despite the high thermal resistance of the nanofibre, which causes a very small change in bending, this relative change is still clearly discernable due to the high sensitivity of the cantilever (Fig. 3b). In Fig. 3c and d, the cantilever deflection is plotted as a
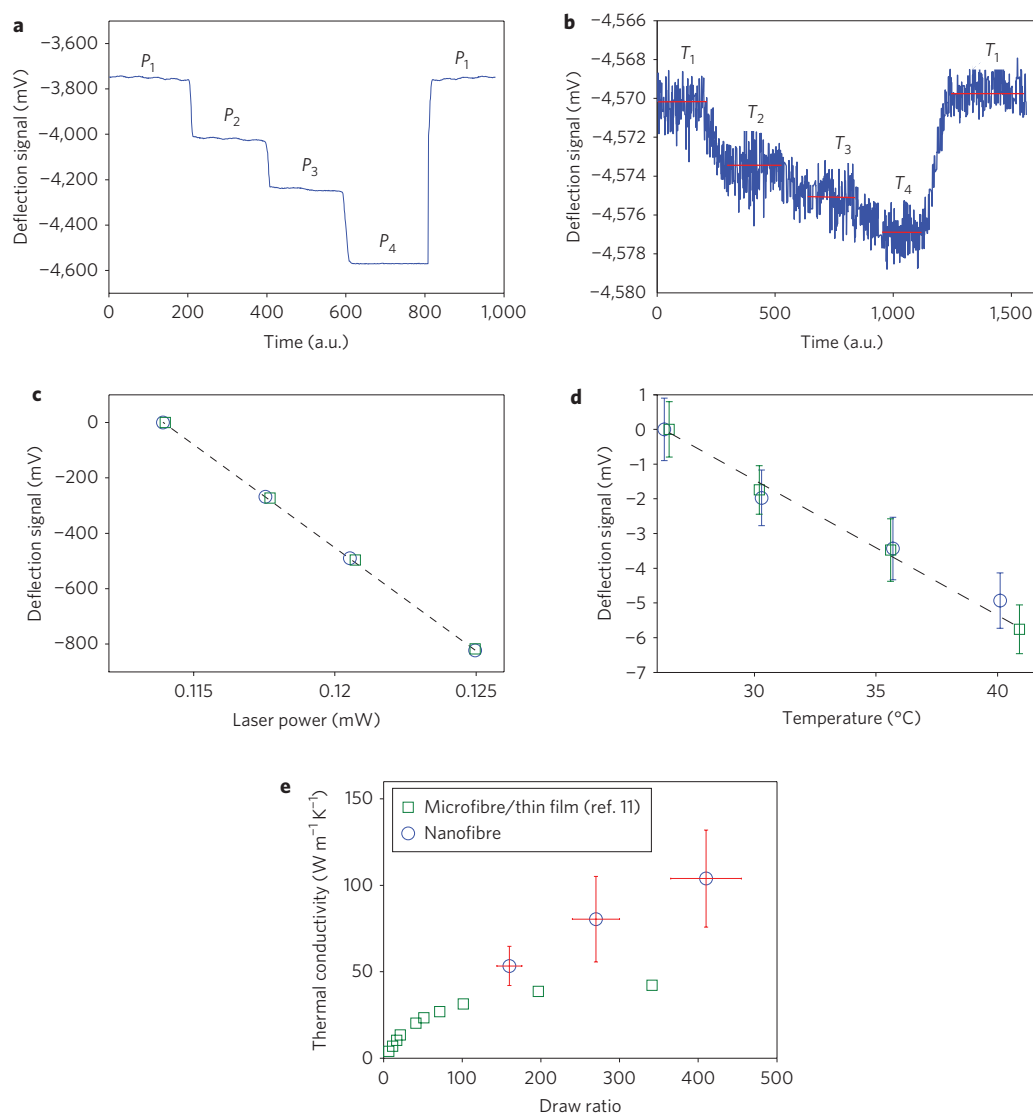
Figure 3 | Measuring the thermal conductivity of individual polyethylene nanofibres. a, Experimental data measured by varying the absorbed power on the end of the AFM cantilever. **b**, Experimental data measured by varying the temperature of the thermocouple. **c**, Reduced deflection signals from **a** versus absorbed power. The data are normalized to the deflection signal at P_1. **d**, Reduced deflection signals of the AFM cantilever from **b** versus the temperature of the thermocouple. The data are normalized to the deflection signal at T_1. The data in **c** and **d** are from two repeated trials on one individual sample, and are marked as blue circles and green squares, respectively. The dashed black lines are the linear fits. The error bar in **c** is ~0.6 mV. **e**, Thermal conductivities of three samples versus their corresponding draw ratios.

function of both the power absorbed by the cantilever (Fig. 3c) and the thermocouple temperature (Fig. 3d) for two repeated measurements on the same sample. Using the slopes extracted from Fig. 3c and d, the nanofibre conductance is obtained from the ratio of both measurements (see Supplementary Information). The length L of each polyethylene nanofibre was measured using optical microscopy and the diameter d was measured using scanning electron microscopy (SEM) at room temperature. Once the geometry was known, the thermal conductivity of each nanofibre was calculated from the conductance. Based on twice or three times repeated measurements for each individual sample, the values obtained were 103.9 ± 28.1 W m^{-1} K^{-1} for sample 1 (with conductance $G = 4.84 \pm 0.94$ nW K^{-1}, diameter $d = 131 \pm 12$ nm and length $L = 290 \pm 10$ μm), 80.4 ± 24.7 W m^{-1} K^{-1} for sample 2 ($G = 5.21 \pm 1.35$ nW K^{-1}, $d = 158 \pm 12$ nm and $L = 300 \pm 10$ μm) and 53.3 ± 11.3 W m^{-1} K^{-1} for sample 3 ($G = 5.59 \pm 0.95$ nW K^{-1}, $d = 197 \pm 12$ nm and $L = 290 \pm 10$ μm). The overall draw ratios for three samples (see Supplementary Information) were estimated

to be ~410 for sample 1, ~270 for sample 2 and ~160 for sample 3. The measured thermal conductivities for the three samples are plotted as a function of draw ratio in Fig. 3e. We can clearly see that the thermal conductivities of the samples increase with increasing draw ratios. Previous results on micrometre-sized fibres showed that thermal conductivity saturates when the draw ratio is above 100 (ref. 11). The results for our nanofibres, however, are not only significantly higher than previous thermal conductivity values, but also do not show saturation, which indicates that there is still room for enhancement.

The highest thermal conductivity of the nanofibres in our work (~104 W m^{-1} K^{-1}) is about three times higher than previously reported values for micrometre-sized fibres and ~300 times that of bulk polyethylene (~0.35 W m^{-1} K^{-1}). This is significant, because the thermal conductivity of condensed matter only spans four orders of magnitude (~0.1 − 1,000). A value of 104 W m^{-1} K^{-1} is higher than that of approximately half of pure metals, including platinum, iron and nickel. Other metals, in

contrast, will have a lower thermal conductivity than pure metals owing to alloy and impurity scattering. In comparison, previous microfibre samples from the literature[16,17] have a thermal conductivity of 30–40 W m^{-1} K^{-1}, which is only in the range of ceramics. To understand the high thermal conductivity of ultra-drawn polyethylene nanofibres, we will briefly describe the effect of drawing on the polyethylene structure based on past efforts on drawing micrometre-sized fibres and thin films[24,25]. Morphological studies of stretched polyethylene samples confirm that, during the initial drawing process (where the draw ratio is small), small crystalline blocks are broken off the crystalline lamellae and incorporated into microfibrils along the draw direction. In these microfibrils, the crystalline blocks are stacked and connected by taut tie molecules (intra-microfibrillar tie molecules), which originate from the partial unfolding of the polyethylene chains. Besides intra-microfibrillar tie molecules, the microfibrils are connected laterally by bridging molecules, which are called inter-microfibrillar tie molecules. Further drawing leads to shear deformation of the microfibrils, resulting in a decrease of the microfibrillar volume fraction and an increase in the number of fully extended interfibrillar tie molecules. Finally, these increasing interfibrillar tie molecules lead to extended chains. The growing chain-extended volume fraction will form a larger average crystal size in the drawing direction. This crystalline region along the drawing direction is the origin for enhanced thermal and mechanical properties. Thus, increasing the length and the volume fraction of the chain-extended crystalline region will enhance the thermal and mechanical properties of ultra-drawn polyethylene samples[15].

In nanofibres, the defect density will decrease, because inherently larger defects such as voids, impurities or large entanglement regions are less likely to be present. Because these types of defects are generally the cause of fracture in the fibre, the successful drawing of a nanofibre is indicative that a higher-quality sample has been fabricated, as is also clear from TEM diffraction patterns (Fig. 1f). Smaller defects, such as small entanglement regions and chain ends, may still exist as a part of the amorphous region, but can be partially transformed to become crystalline during the drawing process. As a result, higher draw ratios are more achievable, and a greater volume fraction of the chain extended crystalline region is more attainable at lower draw ratios for the nanofibres. To convey the importance of scale, the diameter of commercial microfibres is typically 10–25 μm. The diameters of the nanofibres reported in the current work lie between 50 and 500 nm. With identical lengths, the volume of the nanofibre is four orders of magnitude smaller than that of a microfibre; thus, a substantially lower number of defects will exist in the nanofibre than in the microfibre. The improved quality of nanofibres, when compared to microfibres, is also supported by plotting thermal conductivity versus draw ratio (Fig. 3e). The thermal conductivities of the nanofibres are not only much higher than those of micrometre-sized polyethylene materials, but also saturate much more slowly as a function of draw ratios.

When considering a fundamental upper limit of nanofibre thermal conductivity, we would not expect the thermal conductivity of ultra-drawn polyethylene nanofibres to approach the predicted values for a single isolated polyethylene chain. This is because nanofibres consist of many interacting chains, and the chain–chain van der Waals interactions induce phonon–phonon scattering within each chain, which reduces thermal conductivity[26]. These chain–chain interactions, however, can also give rise to a stable orthorhombic crystal structure for polyethylene. Intuitively, we would expect the perfect crystal to have the highest thermal conductivity for a system of interacting polyethylene chains. Thus we conjecture that as bulk polyethylene is stretched, the chain alignment and thermal conductivity increase towards the limit of a single crystal, which serves as a more appropriate upper bounding limit for the thermal conductivity of polyethylene fibres.
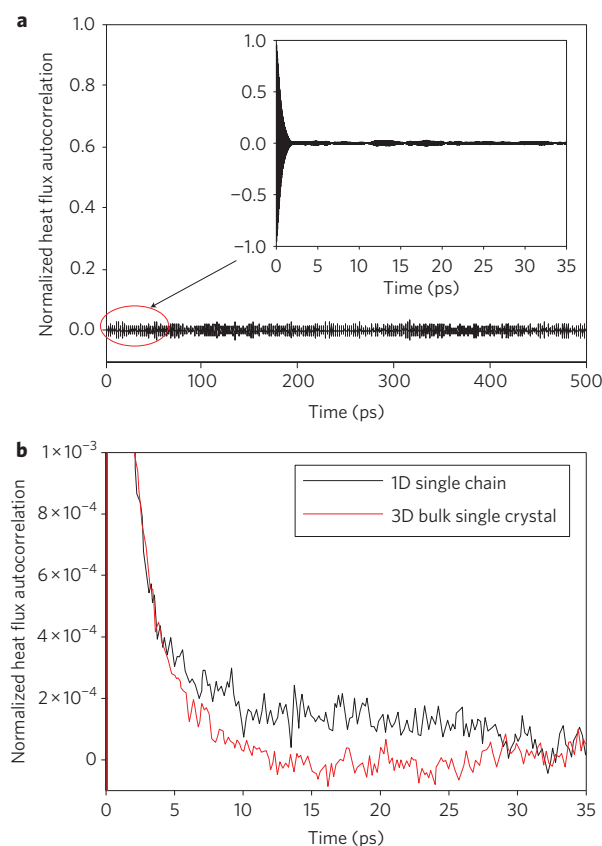

Figure 4 | Molecular dynamics simulation about polyethylene.
a, Normalized heat flux autocorrelation function for a simulation of a single polyethylene chain. **b**, Comparison of normalized heat flux autocorrelation functions between a single polyethylene chain and bulk polyethylene single crystal.

The majority of previous studies qualitatively attributed the thermal conductivity enhancement observed in stretched polyethylene samples to the increase of molecular chain alignment. Here, we used equilibrium molecular dynamics simulations to quantitatively predict the thermal conductivity of a single polyethylene crystal by means of the Green–Kubo approach, $\kappa = (V/k_B T^2) \int_0^\infty \langle Q_z(0) \cdot Q_z(t) \rangle \, dt$, where the thermal conductivity κ is determined by integrating the heat flux autocorrelation function $\langle Q_z(0) \cdot Q_z(t) \rangle$ (see Supplementary Information for simulation details). Our simulation results indicate convergence of the thermal conductivity with respect to simulation time and size, and the average thermal conductivity was 180 ± 65 W m^{-1} K^{-1}. Figure 4a shows the long-term behaviour of the normalized heat flux autocorrelation function of a single molecular chain, and Fig. 4b compares the normalized heat flux autocorrelation function $\langle Q_z(0) \cdot Q_z(t) \rangle$ from a simulation of a single polyethylene chain with that of the full bulk single crystal over a short time range. Here, we can see that the autocorrelation decays more quickly in the bulk crystal, which leads to a lower thermal conductivity. The more rapid decay manifests as enhanced phonon–phonon scattering (loss of correlation) induced by the chain–chain van der Waals interactions.

To the best of our knowledge, our measurements of the thermal conductivity for ultra-drawn polyethylene nanofibres (104 W m^{-1} K^{-1}) represent the highest thermal conductivity reported so far for a polymer. Additionally, we have provided a theoretical estimate for the thermal conductivity of a single polyethylene bulk crystal based on molecular dynamics simulations using the Green–Kubo approach. Our estimate of 180 ± 65 W m^{-1} K^{-1} indicates that it may be possible to

improve the thermal conductivity of polyethylene to a range where it would be competitive with aluminium (235 W m^{-1} K^{-1}). Our experimental results clearly show the potential of using polymers as a cheaper alternative to the conventional metallic heat transfer materials used throughout many industries. This is especially true for applications where directional heat conduction is important, such as in heat-exchanger fins, cell-phone casing, plastic packaging for computer chips and so on. Furthermore, high-thermal-conductivity polymers may also have other technological advantages that can be applied, because they can be lightweight, electrically insulating and chemically stable.

References

1. Sperling, L. H. *Introduction to Physical Polymer Science* (Wiley-Interscience, 2006)
2. Wang, Z. *et al.* Ultrafast flash thermal conductance of molecular chains. *Science* **317,** 787–790 (2007).
3. Wang, R. Y., Segalman, R. A. & Majumdar, A. Room temperature thermal conductance of alkanedithiol self-assembled monolayers. *Appl. Phys. Lett.* **89,** 173113 (2006).
4. Henry, A. & Chen, G. High thermal conductivity of single polyethylene chains using molecular dynamics simulations. *Phys. Rev. Lett.* **101,** 235502 (2008).
5. Baur, J. & Silverman, E. Challenges and opportunities in multifunctional nanocomposite structures for aerospace applications. *MRS Bull.* **32,** 328–334 (2007).
6. Winey, K. I., Kashiwagi, T. & Mu, M. F. Improving electrical conductivity and thermal properties of polymers by the addition of carbon nanotubes as fillers. *MRS Bull.* **32,** 348–353 (2007).
7. Kim, P., Shi, L., Majumdar, A. & McEuen, P. L. Thermal transport measurements of individual multiwalled nanotubes. *Phys. Rev. Lett.* **87,** 215502 (2000).
8. Moniruzzaman, M. & Winey, K. I. Polymer nanocomposites containing carbon nanotubes. *Macromolecules* **39,** 5194–5205 (2006).
9. Huxtable, S. T. *et al.* Interfacial heat flow in carbon nanotube suspensions. *Nature Mater.* **2,** 731–734 (2003).
10. Kanamoto, T., Tsuruta, A., Tanaka, K., Takeda, M. & Porter, R. S. Superdrawing of ultrahigh molecular-weight polyethylene 1. Effect of techniques on drawing of single-crystal mats. *Macromolecules* **21,** 470–477 (1988).
11. Choy, C. L., Wong, Y. W., Yang, G. W. & Kanamoto, T. Elastic modulus and thermal conductivity of ultradrawn polyethylene. *J. Polym. Sci. B* **37,** 3359–3367 (1999).
12. Fermi, E., Pasta, J. & Ulam, S. Studies of nonlinear problems. *Los Alamos Report* LA1940 (1955).
13. Chae, H. G. & Kumar, S. Making strong fibers. *Science* **319,** 908–909 (2008).
14. Smith, P. & Lemstra, P. J. Ultra-high-strength polyethylene filaments by solution spinning/drawing. *J. Mater. Sci.* **15,** 505–514 (1980).
15. Choy, C. L., Fei, Y. & Xi, T. G. Thermal-conductivity of gel-spun polyethylene fibers. *J. Polym. Sci. B* **31,** 365–370 (1993).
16. Poulaert, B., Chielens, J. C., Vandenhende, C., Issi, J. P. & Legras, R. Thermal conductivity of highly oriented polyethylene fibers. *Polym. Commun.* **31,** 148–151 (1990).
17. Fujishiro, H., Ikebe1, M., Kashima, T. & Yamanaka, A. Drawing effect on thermal properties of high-strength polyethylene fibers. *Jpn J. Appl. Phys.* **37,** 1994–1995 (1998).
18. Harfenist, S. A. *et al.* Direct drawing of suspended filamentary micro- and nanostructures from liquid polymer. *Nano Lett.* **4,** 1931–1937 (2004).
19. Nain, A. S., Amon, C. & Sitti, M. Proximal probes based nanorobotic drawing of polymer micro/nanofibers. *IEEE Trans. Nanotechnol.* **5,** 499–510 (2006).
20. Smith, P., Chanzy, H. D. & Rotzinger, B. P. Drawing of virgin ultrahigh molecular-weight polyethylene—an alternative route to high-strength high modulus materials 2. Influence of polymerization temperature. *J. Mater. Sci.* **22,** 523–531 (1987).
21. Barnes, J. R., Stephenson, R. J., Welland, M. E., Gerber, C. & Gimzewski, J. K. Photothermal spectroscopy with femtojoule sensitivity using a micromechanical device. *Nature* **372,** 79–81 (1994).
22. Majumdar, A. Scanning thermal microscopy. *Annu. Rev. Mater. Sci.* **29,** 505–585 (1999).
23. Shen, S., Narayanaswamy, A., Goh, S. & Chen, G. Thermal conductance of bimaterial microcantilevers. *Appl. Phys. Lett.* **92,** 063509 (2008).
24. Peterlin, A. Drawing and extrusion of semi-crystalline polymers. *Coll. Polym. Sci.* **265,** 357–382 (1987).
25. Van Aerle, N. A. J. M. & Braam, A. W. M. A structural study on solid state drawing of solution-crystallized ultra-high molecular weight polyethylene. *J. Mater. Sci.* **23,** 4429–4436 (1988).
26. Morelli, D. T., Heremans, J., Sakamoto, M. & Uher, C. Anisotropic heat-conduction in diacetylenes. *Phys. Rev. Lett.* **57,** 869–872 (1986).

Author contributions

S.S. and G.C. conceived and designed the experiments. S.S. and J.T. performed the experiments. A.H. provided the molecular dynamics simulation. R.Z. contributed TEM analysis. S.S., A.H. and G.C. wrote the paper. All authors discussed the results and commented on the manuscript. G.C. supervised the research.

Additional information

The authors declare no competing financial interests. Supplementary information accompanies this paper at www.nature.com/naturenanotechnology. Reprints and permission information is available online at http://npg.nature.com/reprintsandpermissions/. Correspondence and requests for materials should be addressed to G.C.